NUMERICAL SIMULATION ON MELTING AND SOLIDIFICATION BASED ON LAGRANGIAN APPROACH

Jin-Biao Xiong Hong-Yan Wang Xu Cheng Yan-Hua Yang
School of Nuclear Science and Engineering, Shanghai Jiao Tong University
800 Dongchuan Road Minhang Shanghai 200240 China

xiongjinbiao@sjtu.edu.cn; googlewang@sjtu.edu.cn; chengxu@sjtu.edu.cn; yanhuay@sjtu.edu.cn

ABSTRACT

In case of a severe accident the reactor core may melt and drop into the lower head of pressure vessel. Melting and relocation of corium have great impact on the progress of accident. Based on the MPS (Moving Particle Semi-implicit) method which was proposed by Koshizuka and Oka (1996), a Lagrangian approach is developed to enable the detailed simulation of melting and solidification. Since the surface tension is one of the dominant physics during melting, the potential force surface tension model is implemented into the MPS. Enthalpy-based transition profile of dynamic viscosity near the melting temperature is utilized to reproduce realistic melting behavior. In order to improve the computing efficiency, the implicit calculation scheme is utilized for the viscosity term instead of the original explicit one, which increases the minimum requirement for the time step size. And the Passively Moving Solid (PMS) model is adopted for the coupling calculation of the motion of fluid and solid. In order to verify the implementation of the surface tension model, the square droplet oscillation are simulated and compared with the theoretical solution. The modified MPS method is further validated through comparison with the Wood's metal melting experiment results.

KEYWORDS
Melting, numerical simulation, Lagrangian approach, MPS method

1. INTRODUCTION

During a severe accident the reactor core may melt and drop into the lower head of reactor pressure vessel (RPV). In order to mitigate the severe accident, the corium has to be contained and finally stabilized. Retention strategies have been developed to achieve final stabilization of the corium, e.g. in-vessel retention [1] and core catcher [2]. The behavior of the corium, including its stratification and interaction with structure material, reactor pressure vessel and concrete, is essentially important for the design and assessment of a retention technology. However, the corium behavior can be affected by multiple physics phenomena, including decay heat, melting/liquefaction and solidification. The current analysis approaches for the corium behavior are mainly lumped parameter ones and still confront large uncertainties. For example, a variety of molten pool models have been proposed [1, 3-4], which may lead to very different prediction of heat flux distribution on the outer surface of RPV lower head and result in the uncertainty in in-vessel retention analysis.

Due to the high temperature, experimental investigation on the corium behavior is extremely expensive. The Lagrangian methods, such as the Smoothed Particle Hydraulics (SPH) method [5] and the

Moving Particle Semi-implicit (MPS) method [6], have the intrinsic advantage in tracking free surface and hence can be proper analysis tools for the melting simulation. In this paper, a Lagrangian approach is developed to enable the detailed simulation of melting and solidification based on the MPS method.

2. GOVERNING EQUATION

For the melting and solidification simulation, we need to simulate the motion and heat transfer of fluid and solid parts in a coupled manner. The following equations govern the motion of fluid, i.e.
Continuity equation:

$$\frac{1}{\rho_l}\frac{D\rho_l}{Dt} + \nabla\cdot\left(\vec{u}_l\right) = 0 \tag{1}$$

Momentum equation:

$$\frac{D\vec{u}_l}{Dt} = -\frac{1}{\rho_l}\nabla P_l + \nabla\cdot(\nu_l\nabla\vec{u})_l + \frac{\vec{f}_{s\to l}}{\rho_l} + \frac{\vec{f}_{surf}}{\rho_l} + \vec{g} \tag{2}$$

In a slow melting process the viscosity and surface tension can be significant. The solid part is modelled as rigid body whose motion is governed by the following equations

$$\frac{D\vec{u}_s}{Dt} = \frac{\vec{F}_{col}}{m_s} + \frac{\vec{f}_{l\to s}}{\rho_s} + \vec{g} \tag{3}$$

$$I\frac{D\vec{\omega}_c}{Dt} = \vec{T}_{col} + \vec{T}_{l\to s} + \vec{T}_{other} \tag{4}$$

where the moment of inertia of a rigid body

$$I = \int_V \rho_s r_c^{\,2}\, dV \tag{5}$$

The conjugated heat transfer in the liquid and solid are solved simultaneously

$$\frac{D(\rho H)}{Dt} = \nabla\cdot(k\nabla T) + \ddot{Q} \tag{6}$$

3. SOLUTION ALGORITHM

The solution algorithm of the modified MPS method is shown in Fig. 1. The semi-implicit algorithm adopted in the present study is a fractional-step one slightly different from SMAC[7].

$$\left(\frac{D\vec{u}_l}{Dt}\right)^{viscosity} = \frac{1}{\rho_l}\nabla\cdot(\mu\nabla\vec{u})_l \tag{7}$$

$$\left(\frac{D\vec{u}_l}{Dt}\right)^{other} = \frac{\vec{f}_{surf}}{\rho_l} + \vec{g} \tag{8}$$

$$\left(\frac{D\vec{u}_l}{Dt}\right)^{pressure} = -\frac{1}{\rho_l}\nabla P_l \tag{9}$$

Since the melting material experiences a transit of viscosity from infinitely large to a finite value, in order to avoid the restriction of time step size due to the large viscosity, i.e.

$$\Delta t < \frac{d_p^{\,2}}{\nu}$$

Eq. (7) is solved implicitly. The surface tension and gravity terms in Eq. (7) are explicitly calculated to obtain intermediate the velocity, $\overrightarrow{u_i^{**}}$. For the incompressible fluid, we know

$$\frac{D}{Dt}\left[\nabla\cdot\left(\vec{u}_l\right)\right] = \nabla\cdot\left(\frac{D\vec{u}_l}{Dt}\right) = 0 \tag{10}$$

Hence,

$$\nabla\cdot\left[\left(\frac{D\vec{u}_l}{Dt}\right)^{viscosity} + \left(\frac{D\vec{u}_l}{Dt}\right)^{pressure} + \left(\frac{D\vec{u}_l}{Dt}\right)^{other}\right] = 0 \tag{11}$$

$$\nabla\cdot\left(\frac{1}{\rho}\nabla P\right) = \nabla\cdot\left[\left(\frac{D\vec{u}}{Dt}\right)^{viscosity} + \left(\frac{D\vec{u}}{Dt}\right)^{other}\right] = -\frac{1}{\rho^0}\left(\frac{D^2\rho}{Dt^2}\right)^{vis+other} \tag{12}$$

The pressure Poisson equation, i.e. Eq. (12) is solved implicitly. And the obtained pressure field is used to correct the particle velocity and position. The interaction between the solid and the fluid is simulated with the passively moving solid (PMS) model in which the solid is represented by particles with a fixed relative configuration [8]. Based on the PMS model, the motion solid particle is corrected.

4. DISCRETIZATION

In the MPS method the partial differential equations are discretized based on the particles. A kernel function is utilized to distinguish the interaction intensity between particles at different distance. In the present study the following kernel function is applied

$$w_{ij} = \begin{cases} \frac{r_e}{|\vec{r}_{ij}|} - 1 & 0 \le r \le r_e \\ 0 & \text{if } r_e < r \end{cases} \tag{13}$$

In the three-dimensional simulation we set the cutoff radius $r_e = 2.1d_p$. Here, $d_p$is the particle diameter. The particle number density is defined based on the kernel function

$$\langle n\rangle_i = \sum_{j\neq i} w_{ij} \tag{14}$$

The fluid density is regarded proportional to the particle number density. Hence, when the fluid is incompressible and no particle coalescence or breakup is considered , the particle number density should ideally be constant and equal to initial value, n^0. In the disretization $\langle n\rangle_i$ has been replaced with n^0. The pressure gradient is calculated based on the gradient model which averages the gradients between neighboring particle pairs based on the kernel function. The pressure gradient between two particles can be obtained by $\left(P_i - P_j\right)\vec{\boldsymbol{e}}_{ij}/\left|\vec{\boldsymbol{r}}_{ij}\right|$. Hence the pressure gradient at particle *i* can be calculated with

$$\langle\nabla P\rangle_i = \frac{N_d}{n^0}\sum_{j\neq i}\frac{\left(P_j - P_i\right)}{|\vec{r}_{ij}|} w_{ij}\vec{\boldsymbol{e}}_{ij} \tag{15}$$

where N_d is the number of dimensions in the simulation. In order to stabilize the calculation, Koshizuka proposed

$$\langle\nabla P\rangle_i = \frac{N_d}{n^0}\sum_{j\neq i}\frac{\left(P_j - \hat{P}_i\right)}{|\vec{r}_{ij}|} w_{ij}\vec{\boldsymbol{e}}_{ij} \tag{16}$$

where

$$\hat{P}_i = min\left(P_j, P_i\right)$$

However, the momentum conservation cannot be guaranteed when Eq. (16) is used to discretize the pressure gradient. Hence, the following expression is used instead

$$\langle \nabla P \rangle_i = \frac{N_d}{n^0} \sum_{j \neq i} \frac{(P_j + P_i)\vec{r}_{ij}}{|\vec{r}_{ij}|^2} w_{ij} \tag{17}$$

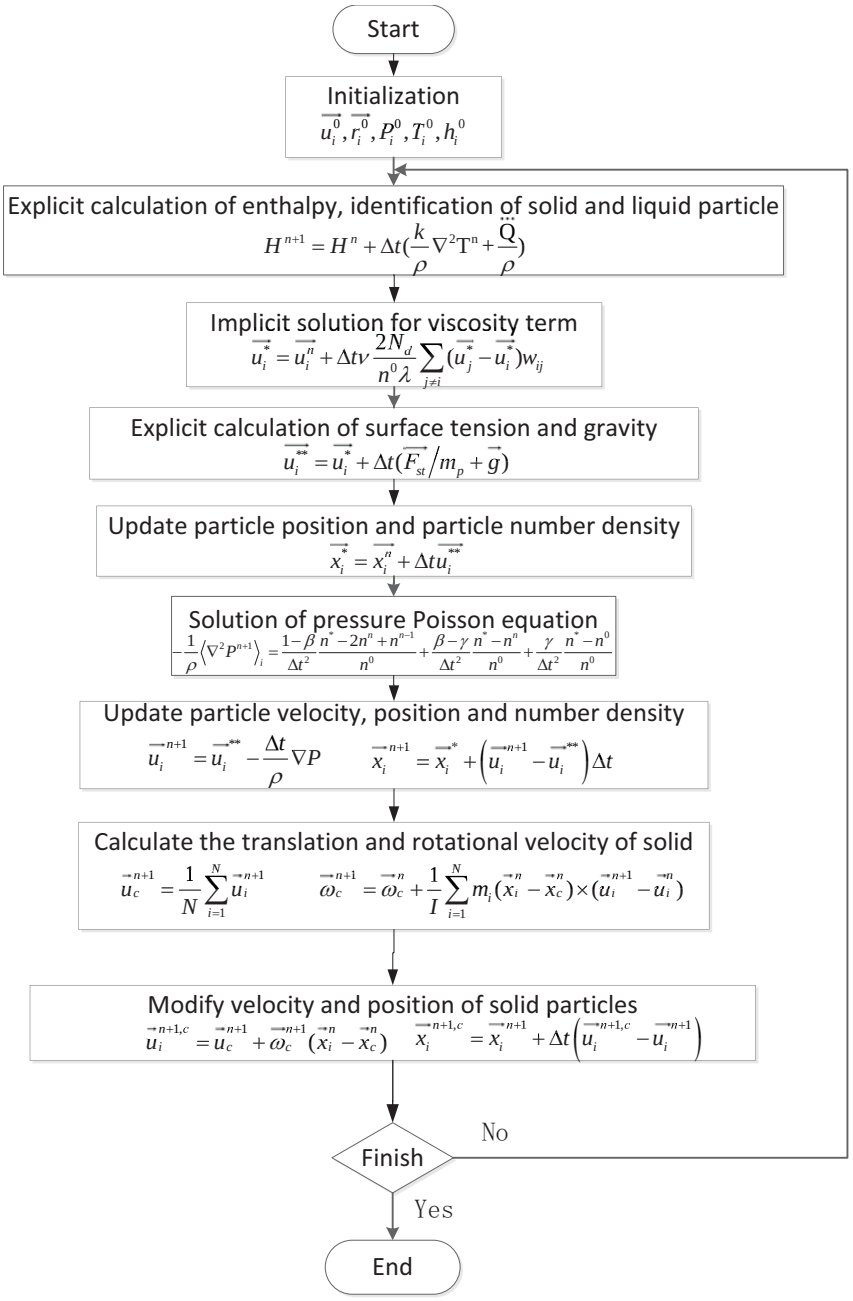

Figure 1 Solution algorithm of the modified MPS method

The Laplacian model

$$\langle \nabla^2 \phi \rangle_i = \frac{2N_d}{\lambda n^0} \sum_{j \neq i} (\phi_j - \phi_i) w_{ij} \tag{18}$$

which was derived based on the diffusion concept [6] has been used to discretize the viscosity term in Eq. (8) and Poisson operator in Eq.(12). The incomplete Cholesky decomposition conjugate gradient

(ICCG) method is utilized when the pressure Poisson equation (PPE) and implicit viscosity term is solved. For better prediction of the pressure distribution, the source term in PPE is discretized as

$$-\frac{1}{\rho^0}\left(\frac{D^2\rho}{Dt^2}\right)^{vis+other} = \frac{1-\beta}{\Delta t^2}\frac{n^* - 2n^n + n^{n-1}}{n^0} + \frac{\beta-\gamma}{\Delta t^2}\frac{n^* - n^n}{n^0} + \frac{\gamma}{\Delta t^2}\frac{n^* - n^0}{n^0} \tag{19}$$

which follows the proposal by Kondo et al. [9].

5. PHYSICS MODELS

5.1 Phase change model

In the present simulation the melting of pure metal is considered. Fig. 2 presents the variation of temperature along with the increasing enthalpy. The liquid mass fraction defined by

$$\varepsilon_i = \begin{cases} 0 & H_i \le H_l \\ \dfrac{H_i - H_s}{H_l - H_s} & H_l < H_i < H_s \\ 1 & H_s \le H_i \end{cases} \tag{20}$$

accounts for the melted/liquefied mass fraction in a particle.

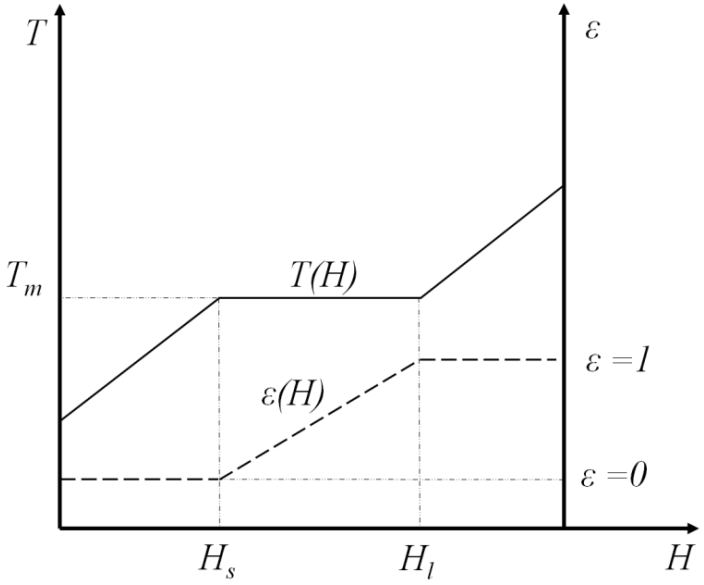

Figure 2 Melting diagram of pure metal

The physics properties are determined based on the liquid mass fraction. One of the important properties is the viscosity which can be regarded as infinitely large for solid. When a solid object is melted, the viscosity drops to a finite value after certain enthalpy increase. The viscosity model proposed by Guo [10] is applied here.

$$\mu_i = \min(\mu_{\max}, \mu_l \exp(\frac{-A(h_i - h_l)}{C_p})) \tag{21}$$

where

$$\mu_{\max} = \mu_l \exp(\frac{-A(h_{\varepsilon=0.375} - h_l)}{C_p}) \tag{22}$$

5.2 Surface tension model

The potential force surface tension model proposed by Kondo [11] is implemented in the modified MPS code. Kondo's surface tension model adopted the concept of inter-particle potential energy. The potential force becomes repellent when the distance between two particles is shorter than the particle diameter, while it becomes attraction force when particle distance is longer than the particle diameter. The potential energy between two particles is defined by

$$E_p\left(\left|\vec{r}_{ij}\right|\right)=\begin{cases}\dfrac{C}{3}\left(\left|\vec{r}_{ij}\right|-1.5d_p+0.5r_e\right)\left(\left|\vec{r}_{ij}\right|-r_e\right) & \left|\vec{r}_{ij}\right|<r_e\\ 0 & \left|\vec{r}_{ij}\right|\geq r_e\end{cases} \tag{23}$$

For two fluid particles the constant in the above equation is given by

$$C_f=\frac{6\sigma {d_p}^2}{\sum_{i\neq j}\left(\left|\vec{r}_{ij}\right|-1.5d_p+0.5r_e\right)\left(\left|\vec{r}_{ij}\right|-r_e\right)} \tag{24}$$

Between fluid and solid particles, the constant is given by

$$C_{fs}=\frac{C_f}{2}(1+\cos\theta) \tag{25}$$

where θ is the contact angle of fluid on a solid surface. The inter-particle force exerted by particle j on particle i can be expressed by

$$\vec{f}_{j\to i}=\frac{\partial E_p}{\partial\left|\vec{r}_{ij}\right|}\vec{e}_{ij}=C(\left|\vec{r}_{ij}\right|-r_e)(r_{\min}-\left|\vec{r}_{ij}\right|)\vec{e}_{ij} \tag{26}$$

The acceleration due to surface tension force is given by

$$\left(\frac{D\vec{u}_l}{Dt}\right)^{surf}=\frac{\sum_{i\neq j}\vec{f}_{j\to i}}{m_i} \tag{27}$$

5.3 Passively moving solid model

The passively moving solid (PMS) model proposed by Koshizuka et al. [8] is utilized to avoid the explicit calculation of interaction force between solid and fluid. In this model the solid particle is first treated as a fluid particle to obtain preliminary velocity, $\vec{u}^{n+1,p}$. The motion of each solid part includes translational and rotational one. The translational velocity is given by

$$\vec{u}_c^{\,n+1}=\frac{1}{N}\sum_{i=1}^{N}\vec{u}_i^{\,n+1} \tag{28}$$

The angular velocity

$$\vec{\omega}_c^{\,n+1}=\vec{\omega}_c^{\,n}+\frac{1}{I}\sum_{i=1}^{N}m_i(\vec{x}_i^{\,n}-\vec{x}_c^{\,n})\times(\vec{u}_i^{\,n+1}-\vec{u}_i^{\,n}) \tag{29}$$

where N is the total particle number in a solid piece. The gravity center of the solid is defined by

$$\vec{x}_c = \frac{\sum_{i=1}^{N} m_i \vec{x}_i}{\sum_{i=1}^{N} m_i} \tag{30}$$

The inertial

$$I = \sum_{i=1}^{N} m_i \left(\vec{x}_i^{\,n} - \vec{x}_c^{\,n} \right)^2 \tag{31}$$

The velocity and position of solid particle is corrected with the translational velocity and angular velocity obtained from Eq. (28) and (29).

$$\vec{u}_i^{\,n+1,c} = \vec{u}_c^{\,n+1} + \vec{\omega}_c^{\,n+1} \left(\vec{x}_i^{\,n} - \vec{x}_c^{\,n} \right) \tag{32}$$

$$\vec{x}_i^{\,n+1,c} = \vec{x}_i^{\,n+1} + \Delta t \left(\vec{u}_i^{\,n+1,c} - \vec{u}_i^{\,n+1} \right) \tag{33}$$

6. MODEL VERIFICATION

6.1 Transient heat conduction

In order to verify that the heat transfer model has been properly implemented, the one-dimensional transient heat conduction in two solid materials is simulated with the modified MPS code. The initial configuration of the solved problem is shown in Figure 3. The interface between two materials locates at x=0. The thickness of each material is 3cm. The initial temperature of material A is 300 ℃, while 600℃ for material B. The material properties are given in Table 1. The analytical solution of temperature variation for the above mention problem can formulated as

$$T_A(t,x) = T_{A,t=0} + (T_{x=0} - T_{A,t=0}) \left\{ 1 - erf\left(\frac{-x}{2\sqrt{\alpha_A t}} \right) \right\} \tag{34}$$

$$T_B(t,x) = T_{B,t=0} + (T_{x=0} - T_{B,t=0}) \left\{ 1 - erf\left(\frac{-x}{2\sqrt{\alpha_B t}} \right) \right\} \tag{35}$$

where

$$T_{x=0} = \frac{\sqrt{\rho_A C_{p,A} k_A} T_{B,t=0} + \sqrt{\rho_B C_{p,B} k_B} T_{B,t=0}}{\sqrt{\rho_A C_{p,A} k_A} + \sqrt{\rho_B C_{p,B} k_B}} \tag{36}$$

The numerical solution by the modified MPS method is compared with the analytical solution in Figure 4. The good agreement indicates that the explicit solution of energy equation can predict the heat transfer when the time step is well controlled.

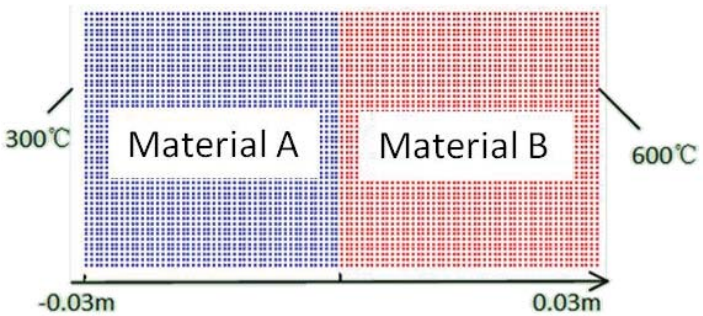

Figure 3 Initial condition of transient heat conduction

Table 1 the physical properties of two materials

	Material A	Material B
Density (kg/m^3)	8000	8000
Heat capacity (J/(kg-K))	499	500
Heat conductivity (W/(m.K))	30	3

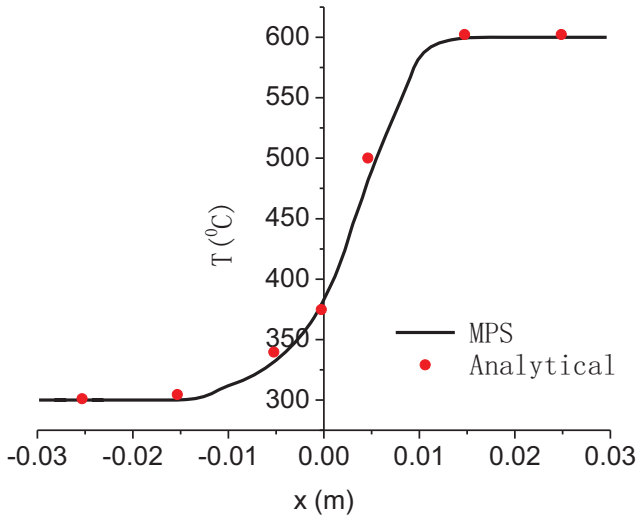

Figure 4 Comparison between numerical and analytical solutions

6.2 Droplet behavior

In order to evaluate the implemented surface tension model, a two-dimensional droplet oscillation problem is solved. The droplet has the initial shape of square and starts to oscillate due to the surface tension. In our simulation the length of the side of the initial square is 75 mm. The side is represented by 30 particles and the total number of the particles is 900. Density of liquid is 798 kg/m^3. Surface tension is 2.361×10^{-2} N/m. The theoretical oscillation period is 1.36 s.

Figure 5 presents the simulation results which shows the oscillation period is about 2 s which is longer than the theoretical value.

To demonstrate the capability to simulate the contact angle, the attachment of a droplet on a solid wall is simulated with the modified MPS method. The simulation result is shown in Figure 6. It is shown that the contact angle can be well simulated with the modified code.

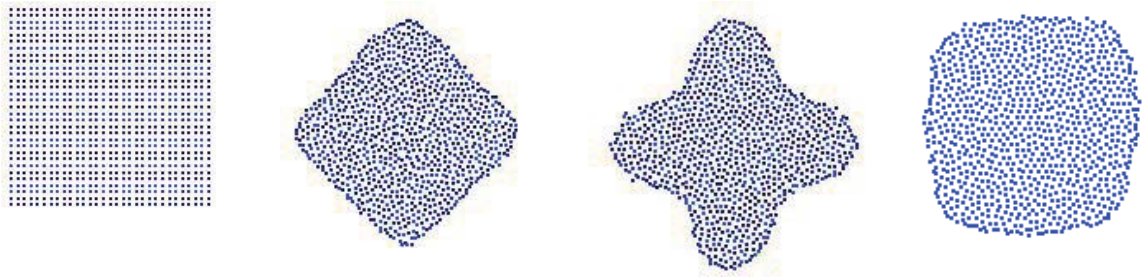

t=0.00s t=0.75s t=1.5s t=2.00s

Figure 5 Simulation result of droplet oscillation

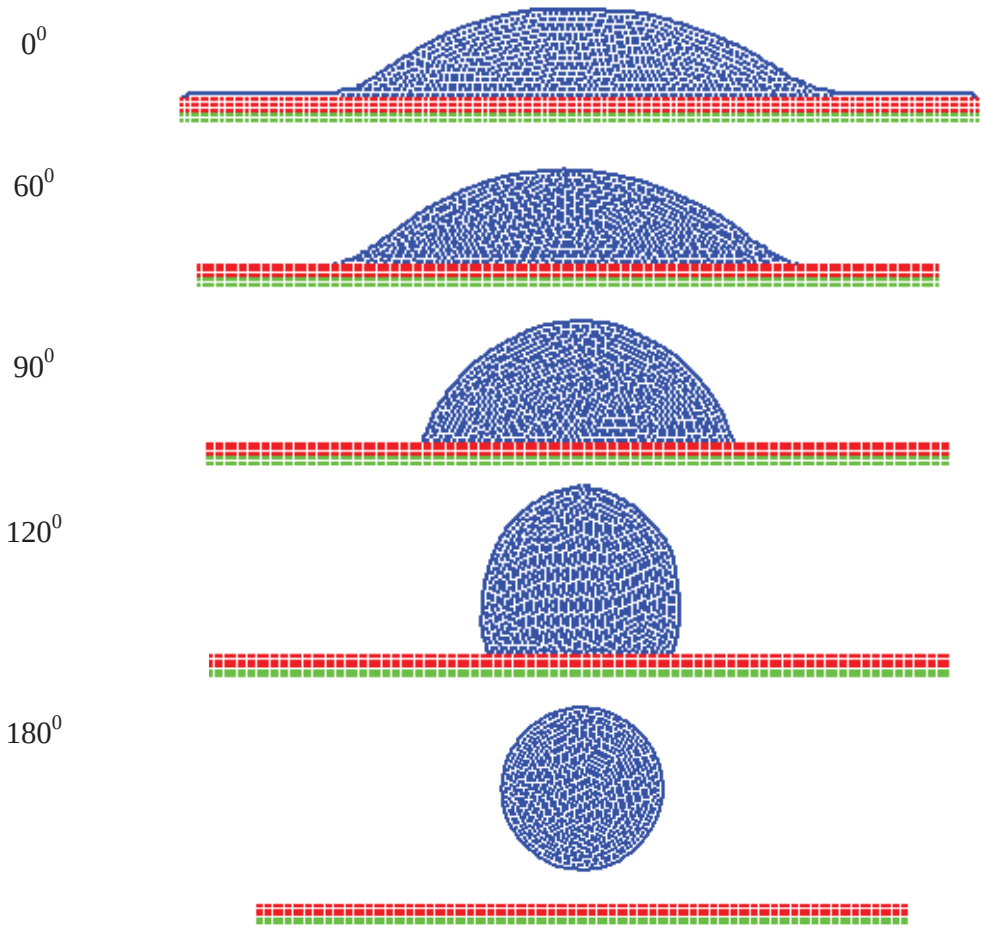

Figure 6 Calculation result of droplet behavior with different contact angle on solid wall

7. MELTING SIMULATION

The melting experiment carried out by Guo et al. [10] is simulated with the modified code. In their experiment the Wood's Metal is heated from the bottom with a copper plate at constant temperature. The properties of the Wood's metal is given in Table 2 . Figure 7 shows the initial geometry of the Wood's metals which is a cubic with the side length of 2 cm. The copper plate locates below Z=0. In the simulated case the cooper plate temperature is 350 ^{o}C. Hence, five layers of wall particles with constant temperature is set below the plane Z=0. The initial temperature of the Wood's metal is 27 ^{o}C. The simulation neglects the radioactive and convective heat transfer with the ambient and considers only the heat conduction between the Wood's Metal and the copper plate. The particle size utilized in the current simulation is 0.1 mm and the time step size is set as $1x10^{-4}$ s.

Since the contact angle of the molten Wood's metal on the copper surface and the Wood's metal surface is not exactly measured. A sensitivity investigation on the effect of contact angle is carried out with the contact angle of 90^{o}, 120^{o} and 150^{o}. The simulation result is shown in Figure 8 which indicates that a larger contact leads to slower spreading of the molten metal and thicker molten metal layer. Comparing with the experimental photo given by Guo et al. [10] the contact angle $\theta = 120^{0}$ is adopted in the further analysis.

Table 2 Physical properties of Wood's metal [10]

Melting temperature	78.8 ^{o}C	
Latent heat	47.5x10^{3} kJ/kg	
Density	8528 kg/m^{3}	
Specific heat capacity	Liquid	Solid
	190 J/(kg$\cdot$ ^{o}C)	168.5 J/(kg$\cdot$ ^{o}C)
Heat conductivity	12.8 W/(m$\cdot$K)	9.8 W/(m$\cdot$K)
Dynamic viscosity	2.4x10^{-3} Pa$\cdot$S	
Surface tension	0.1 N/m	

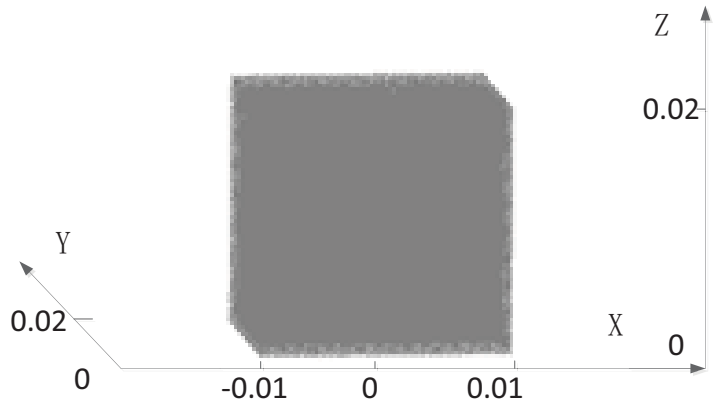

Figure 7 Initial configuration of particles

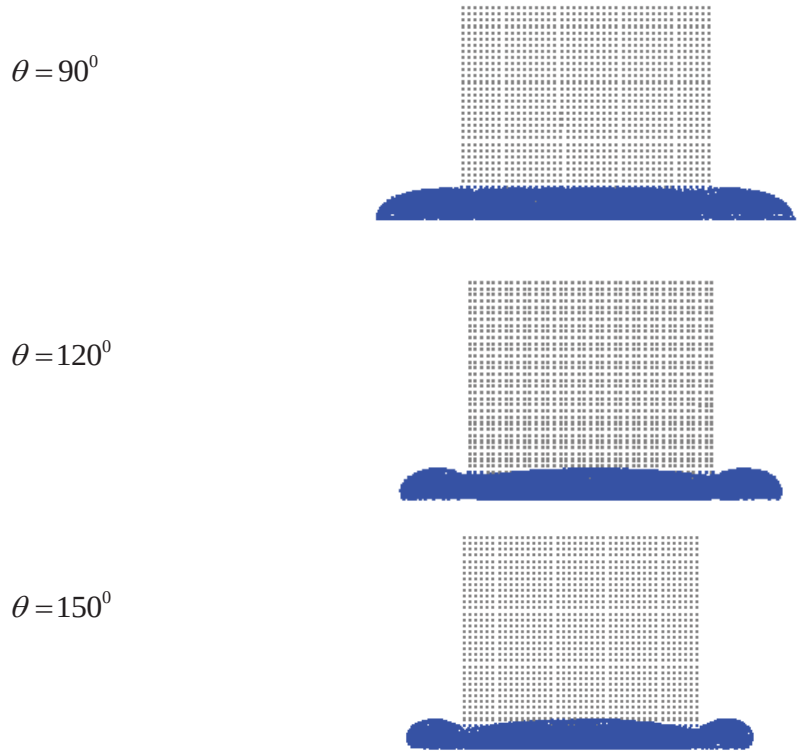

Figure 8 Effect of contact angle on melting behavior

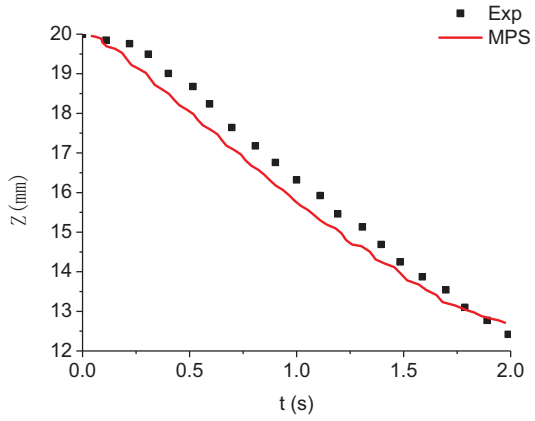

Figure 9 Variation of top height of the solid piece

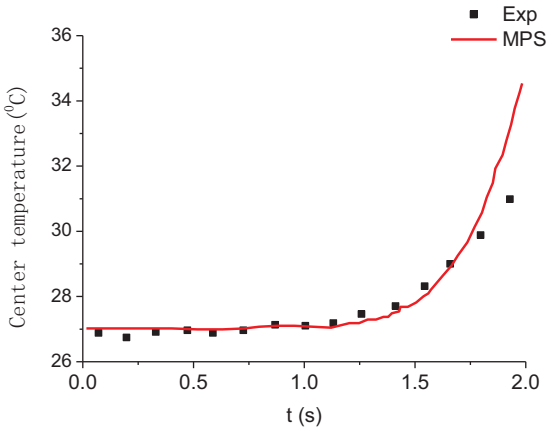

Figure 10 Center temperature of the solid piece

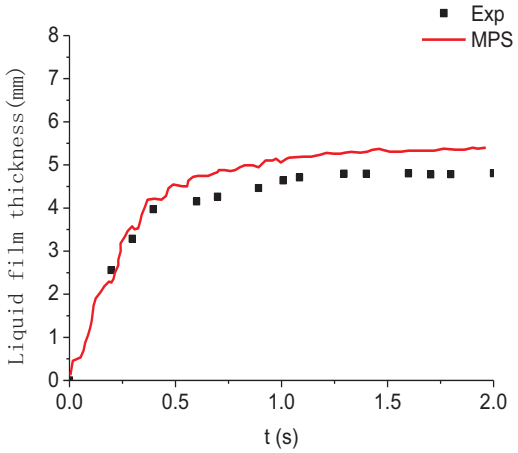

Figure 11 Variation of liquid film thickness

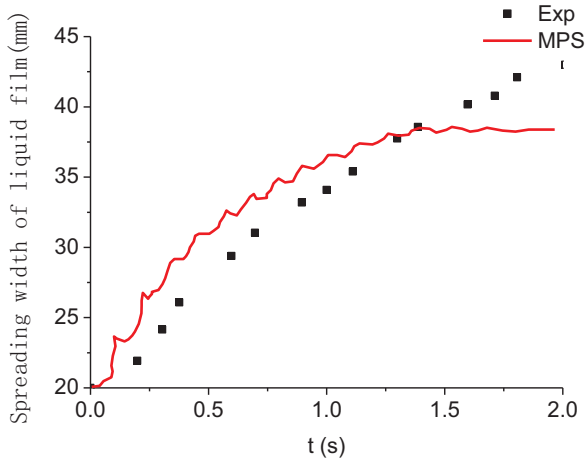

Figure 12 Spreading width of liquid film

Figure 9 through 12 compare the simulation results with the experimental measured data which reflect the motion and heat transfer of the melted and solid Wood's metal. It can be concluded that the modified MPS code can be utilized to simulate the melting process.

8. CONCLUSION

The original MPS (Moving Particle Semi-implicit) method is further developed to enable the detailed simulation of the melting process. The improvements for the original MPS include: 1) The additional energy equation is solved to simulate the heat transfer process; 2) Several surface tension models are compared to determine the most appropriate one for melting simulation; 3) The enthalpy-based transition profile of viscosity near the melting temperature is implemented in order to reproduce more realistic melting behavior. 4) The implicit calculation scheme is utilized for the viscosity term in place of the original explicit one, which augments the time step size and hence improves the computing efficiency; 5) The Passively Moving Solid (PMS) model is adopted for the coupling calculation of the motion of fluid and solid.

The one-dimensional unsteady heat transfer and square droplet oscillation are respectively used to verify the implementation of the heat transfer model and surface tension model. Furthermore, the modified

3D MPS method is validated by comparing the experiment results of Wood's metal melting with the numerical result. Based on the validation it can be concluded that the modified MPS code can be utilized to simulate the melting process.

ACKNOWLEDGEMENT

The authors would like to acknowledge the financial support from Shanghai Pujiang Program (No. 13PJ1404900) and thanks Professor Seiichi Koshizuka from the University of Tokyo for providing us the original MPS code.

NOMENCLATURE

$\vec{e}_{ij}$	Unit vector from particle i to particle j
$\vec{f}$	Force on unit volume, N/m^3
$\vec{F}$	Force, N
$\vec{g}$	Gravity acceleration, m/s^2
H	Specific enthalpy, J/kg
k	Heat conductivity, W/(m-K)
n	Particle number density
N_d	Number of dimension
P	Pressure, Pa
$\ddot{Q}$	Volumetric heat source, W/m^3
r_c	Distance to the gravity center, m
r_e	Cutoff radius, m
$\vec{r}_{ij}$	$\vec{x}_i - \vec{x}_j$, m
t	Time, s
T	Temperature, K
w_{ij}	Kernel function
$\vec{x}_i$	Coordinate vector of the *i*th particle, m
	Greek letter
α	Heat diffusivity, m^2/s
β	Blending coefficient
ε	Mass fraction of liquid in one particle
γ	Blending coefficient
$\vec{\omega}$	Angular acceleration, rad/s^2
ρ	Density, kg/m^3

REFERENCES

[1] T. G. Theofanous, *et al.*, "In-vessel coolability and retention of a core melt," *Nuclear Engineering and Design*, vol. 169, pp. 1-48, 1997.

[2] M. Fischer, "The severe accident mitigation concept and the design measures for core melt retention of the European Pressurized Reactor (EPR)," *Nuclear Engineering and Design,* vol. 230, pp. 169-180, 2004.

[3] J. L. Rempe, *et al.*, "Potential for AP600 in-vessel retention through ex-vessel flooding," INEEL/EXT--97-00779, 1997.

[4] O. Kymäläinen, *et al.*, "In-vessel retention of corium at the Loviisa plant," *Nuclear Engineering and Design,* vol. 169, pp. 109-130, 6/1/ 1997.

[5] J. J. Monaghan, "Simulating Free Surface Flows with SPH," *Journal of Computational Physics,* vol. 110, pp. 399-406, 1994.

[6] S. Koshizuka and Y. Oka, "Moving-Particle Semi-Implicit Method for Fragmentation of Incompressible Fluid," *Nuclear Science and Engineering,* vol. 123 pp. 421-434, July 1996 1996.

[7] A. A. Amsden and F. H. Harlow, "The SMAC method: a numerical technique for calculating incompressible fluid flows," 1970.

[8] S. Koshizuka, *et al.*, "Numerical analysis of breaking waves using the moving particle semi-implicit method," *International Journal for Numerical Methods in Fluids,* vol. 26, pp. 751–769, 1998.

[9] M. Kondo and S. Koshizuka, "Improvement of stability in moving particle semi-implicit method," *International Journal for Numerical Methods in Fluids,* vol. 65, pp. 638-654, 2011.

[10] L. Guo, *et al.*, "Numerical simulation of rheological behavior in melting metal using finite volume particle method," *Journal of Nuclear Science and Technology,* vol. 47, pp. 1011-1022, 2010.

[11] M. Kondo, *et al.*, "Surface tension model using inter-particle force in particle method," presented at the The 5th Joint ASME/JSME Fluids Engineering Conference, San Diego, California USA, 2007.